*inorganics*

MDPI

*Review*

# Polyoxometalate–Polymer Composites with Distinct Compositions and Structures as High-Performance Solid Electrolytes

**Takeru Ito**

Department of Chemistry, School of Science, Tokai University, Hiratsuka 259-1292, Japan; takeito@tokai.ac.jp

**Abstract:** Solid electrolytes, including polymer electrolytes, are a promising option for improving the performance of environmentally friendly batteries such as rechargeable lithium-ion batteries or fuel cells. Hydrogen–oxygen fuel cells producing only water under power generation are attracting widespread attention, and they need proton conductors as electrolytes. Fluoropolymer electrolytes such as Nafion® have been utilized for hydrogen–oxygen fuel cells below 100 °C; however, they are not applicable over the working temperature. Therefore, other types of polymer electrolytes are demanded for hydrogen–oxygen fuel cells. Polyoxometalate (POM) inorganic clusters are known as proton conductors and are utilized to prepare POM–polymer composites for solid electrolyte application. In such POM–polymer composites, distinct compositions and structures are significant for improving the performance of proton conductivity. Recently, POM–polymer composites with distinct compositions and structures have been synthesized to obtain high proton conductivity. The key factor is to use single-crystalline compounds. Here, several examples are overviewed by classifying them into three categories: (i) single-crystalline POM–polymer composites, (ii) organically modified POM (org-POM) polymers, and (iii) POM hybrid polymers using polymerizable cations. The application of proton-conductive solid electrolytes is focused on.

**Keywords:** solid electrolyte; proton conductivity; inorganic–organic; polymer; polyoxometalate (POM); polyoxometalate–polymer (POM–polymer) composite; distinct composition and structure; single crystalline

check for updates

Academic Editors: Torben R. Jensen and Yuping Wu

Received: 14 January 2025
Revised: 18 February 2025
Accepted: 3 March 2025
Published: 5 March 2025

**Citation:** Ito, T. Polyoxometalate–Polymer Composites with Distinct Compositions and Structures as High-Performance Solid Electrolytes. *Inorganics* **2025**, *13*, 75. https://doi.org/10.3390/inorganics13030075

**Copyright:** © 2025 by the author. Licensee MDPI, Basel, Switzerland. This article is an open access article distributed under the terms and conditions of the Creative Commons Attribution (CC BY) license (https://creativecommons.org/licenses/by/4.0/).

## 1. Introduction

Efficient energy conversion and usage are crucial for realizing sustainable societies. The development of environmentally friendly batteries is an urgent issue. As for rechargeable batteries, lithium-ion batteries have already been industrialized [1,2], and the development of sodium-ion batteries as next-generation rechargeable batteries is underway [3,4]. Other environmentally friendly batteries include fuel cells, such as hydrogen–oxygen fuel cells producing only water for power generation [5]. In hydrogen–oxygen fuel cells, hydrogen gas is converted to a proton with the help of a platinum catalyst, and the proton moves in the electrolyte to react with oxygen to produce water. The electrolyte should be a proton conductor, desirably used in the solid state with respect to safety problems [6–9]. Commercial hydrogen–oxygen fuel cells employ polymer electrolytes [5]. Fluoropolymers with deprotonatable sulfo groups such as Nafion® are typically used in the form of a membrane. These fluoropolymers behave as superior proton conductors only in the presence of water molecules below a working temperature of 100 °C for hydrogen–oxygen fuel

cells. The working temperature should be higher, over 100 °C, to prevent poisoning from the platinum catalyst and to improve the reaction efficiency. Additionally, the fluorine contained in the fluoropolymer electrolytes may be harmful to the environment. Therefore, proton-conductive and fluorine-free polymer materials working over 100 °C are required as solid electrolytes for hydrogen–oxygen fuel cells. Although several systems have been reported [10–17], polymer electrolytes exhibiting higher performance are in demand.

For enhancing the conductive properties of polymer materials, conductive polyoxometalate inorganic clusters (POMs) are promising candidates. POMs are molecular oxide anions with distinct structures [18–24]. POMs contain many transition-metal atoms in the $d^0$ state, and have electrochemical characteristics beneficial to the conductive properties: they behave as electron reservoirs or as reactive components in multi-electron reactions. Their physicochemical properties can be designed and controlled by changing the molecular structures and by converting the counter cations [22–24]. Heteropolyacids, POMs with protons as counter cations, are highly proton-dissociative, and well known as "superacids". Heteropolyacids exhibit proton conductivity in the presence of water vapor [25], but they are hygroscopic and their durability in the presence of water vapor should be improved. Their proton conductivity decreases under heating due to the loss of water molecules, which is a similar disadvantage to that of proton-conductive fluoropolymers. Cation exchange and hybridization with polymer matrices are possible options for the application. Several proton-conductive POM compounds [25–36] and composites with polymers [37–50] have been reported to date. The hybridization of POMs with polymer matrices is usually based on simple combination to enhance the proton conductivity at working temperatures over 100 °C. However, precise control of compositions and structures is rather difficult to achieve, which could be a drawback for the emerging high proton conductivity.

Utilizing single-crystalline materials is an effective way to prepare POM–polymer composites with distinct compositions and structures. Single crystals can be ambiguously revealed with respect to their chemical compositions and molecular structures. Synthesizing single-crystalline POM–polymer hybrids leads to the construction of POM–polymer composites having distinct compositions and structures. Another promising method is to use single-crystalline polymerizable POM monomers for the preparation of well-defined POM–polymer composites.

Recent progress in synthetic methodology has enabled the successful preparation of single-crystalline POM–polymer composites and composites using single-crystalline polymerizable POMs. They possess distinct compositions and structures and exhibit high proton conductivity, and they could be candidates as alternatives to the conventional fluoropolymer electrolytes. Such POM–polymer composites can be categorized into three classes (Figure 1): (i) Single-crystalline POM–polymer composites (Figure 1a). POM and polymer matrices that are effective for proton conductivity are hybridized to obtain single crystals. (ii) Organically modified POM (denoted as "org-POM") anions (Figure 1b). org-POMs with polymerizable groups can be precisely synthesized, and can sometimes be obtained as single crystals. (iii) Single-crystalline POMs hybridized with polymerizable cations (Figure 1c). The combination of POMs and polymerizable cations is variable. These three types of POM–polymer composites are overviewed below regarding the synthetic method, structure, and characteristics of proton conductivity.

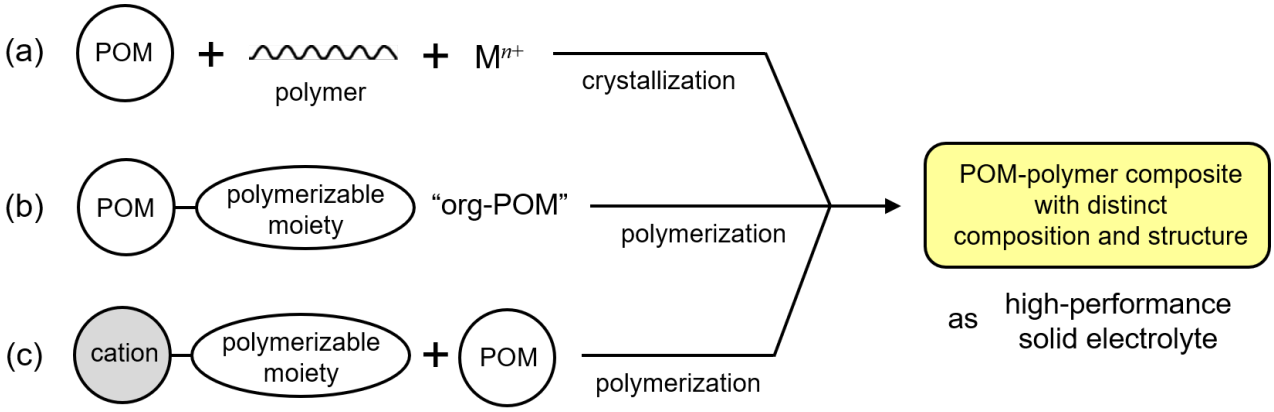



**Figure 1.** POM–polymer composites with distinct compositions and structures as high-performance solid electrolytes: (**a**) single-crystalline POM–polymer composites; (**b**) organically modified POM (org-POM) polymers; (**c**) POM hybrid polymers using polymerizable cations.

## 2. Single-Crystalline POM–Polymer Composites

Conventional POM–polymer composites have been prepared by mixing POM compounds and polymer matrices [37–40]. Neutral POM compounds can be added to polymers as conductive components [44–47]. POM anions can also be combined with polymers with a cationic moiety by using electrostatic interactions [48]. Polymer matrices can be constructed by sol–gel reactions with coexisting POM species [49,50]. All these methods enable the facile preparation of POM–polymer composites and have been widely investigated. However, as mentioned above, the precise design and control of chemical compositions and material structures are rather difficult to achieve at a molecular level.

To solve this problem, utilizing single-crystalline materials is a promising option. Recently, simply mixing POMs with polymer matrices led to single-crystalline POM–polymer composites (Figures 2 and 3) [51–58]. The conductive mechanisms have been discussed in detail. In 2016, Tsuboi et al. found that Keggin-type polyoxotungstate ($[PW_{12}O_{40}]^{3-}$ ($PW_{12}$) and $[SiW_{12}O_{60}]^{4-}$ ($SiW_{12}$)) formed single-crystalline composites with poly(ethylene glycol) (PEG), which is effective for proton conductivity [51]. In a typical synthesis, a heated aqueous solution containing dodecatungstophosphoric acid ($H_3PW_{12}O_{40}$, H-$PW_{12}$), PEG, and $CsNO_3$ gave colorless crystals of a POM-PEG composite (Figure 3a). The negative charge of POM was compensated with $Cs^+$ and residual $H^+$. The crystal structure was formed by an inorganic framework consisting of $PW_{12}$ and $Cs^+$. There were one-dimensional (1D) channels with diameters of ca. 6 Å × 8 Å along the *c*-axis, plausibly holding PEG and $H_2O$ molecules. The atomic positions of the PEG molecules could not be determined solely by single-crystal X-ray diffraction, but their presence was confirmed by elemental analyses and spectroscopic measurements. The POM-PEG composite (Cs-$PW_{12}$-PEG1000) exhibited a proton conductivity of $1.2 \times 10^{-5}$ S cm$^{-1}$ at 170 °C (443 K) under anhydrous (non-humidified) conditions (Figure 3a). Using POMs with a larger molecular size, such as Dawson-type POMs ($[\alpha\text{-}P_2W_{18}O_{62}]^{6-}$, $P_2W_{18}$), resulted in a moderate anhydrous proton conductivity of $1.3 \times 10^{-4}$ S cm$^{-1}$ at 150 °C (423 K) (CsK-$P_2W_{18}$-PEG400, Figure 3b) [52]. Preyssler-type $[Bi(H_2O)P_5W_{30}O_{110}]^{12-}$ ($BiP_5W_{30}$) and the PEG system exhibited a proton conductivity of $4.0 \times 10^{-4}$ S cm$^{-1}$ at 95 °C (368 K) [53]. Larger POMs seem to enhance the anhydrous proton conductivity due to the enlargement of the spaces between POM anions, which enables effective segmental movement of PEG chains and/or the formation of a hydrogen bonding network.

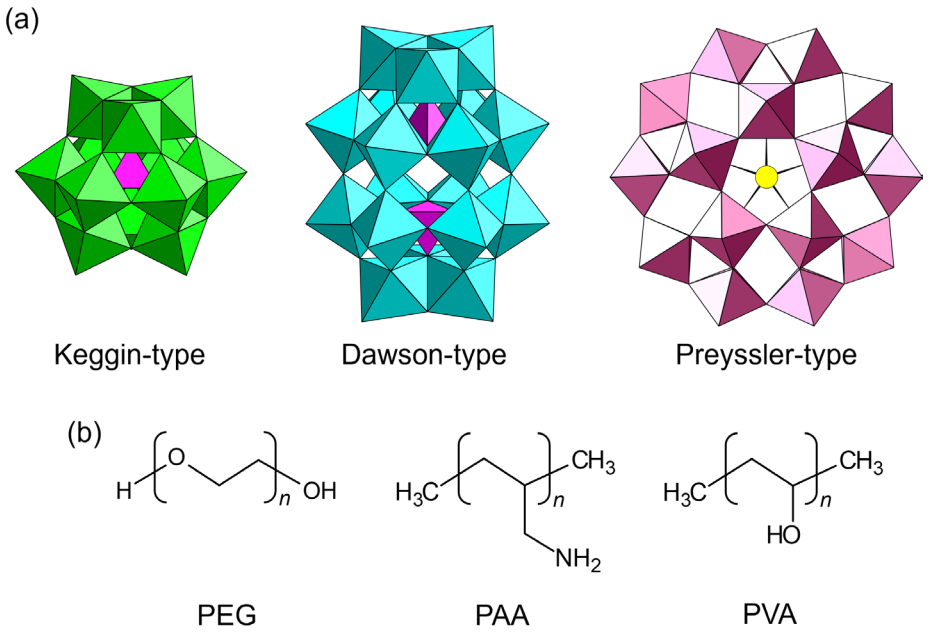



**Figure 2.** Chemical components utilized for the synthesis of single-crystalline POM–polymer composites: (**a**) POM anions; (**b**) polymer matrices. PEG: poly(ethylene glycol); PAA: poly(allylamine); PVA: poly(vinyl alcohol).

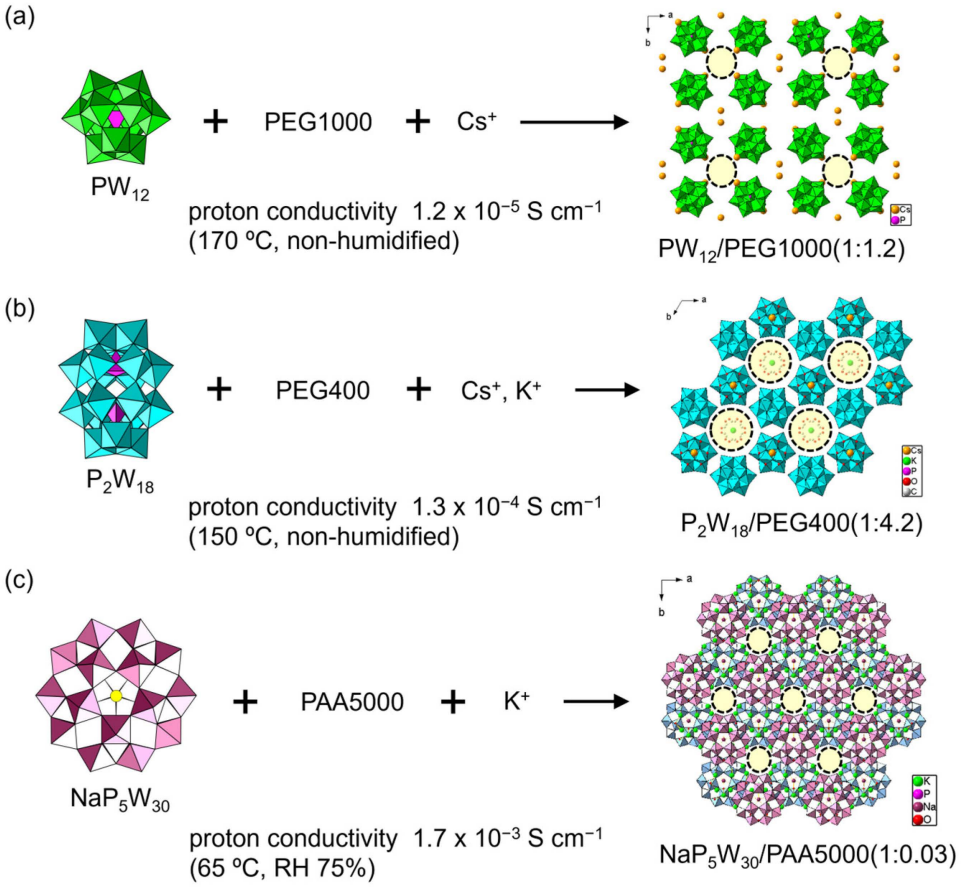



**Figure 3.** Single-crystalline POM–polymer composites. The number of polymer components represents the average molecular weight. One-dimensional channels are indicated by dashed circles. The POM–polymer ratios in the composite are indicated in the figure: (**a**) Keggin-type POM/PEG system; (**b**) Dawson-type POM/PEG system; (**c**) Preyssler-type POM/PAA system. The color of Preyssler-type POMs is changed for clarity.

POM-PEG composites were rather unstable as solid electrolytes under humidified conditions due to solubility problems. Changing the polymer matrix to poly(allylamine) (PAA) drastically enhanced the proton conductivity, since protonated PAA can serve as a cationic species interacting with POM anions to stabilize the crystal structures of POM–polymer composites [53–57]. An inorganic framework constructed from larger Preyssler-type POMs and counter metal cations worked as an effective host for a PAA matrix. The PAA position was not decided by single-crystal X-ray measurements derived from severe disordering. In the $[Na(H_2O)P_5W_{30}O_{110}]^{14-}$ ($NaP_5W_{30}$) and $K^+$ inorganic framework (K-$NaP_5W_{30}$-PAA5000), a 1D channel structure filled with PAA molecules was formed along the *c*-axis, and exhibited a high proton conductivity of $1.7 \times 10^{-3}$ S cm$^{-1}$ at 65 °C (338 K) under mild humidity (RH 75%) (Figure 3c) [53]. Changing POM species to $BiP_5W_{30}$ enhanced the conductivity to the order of ~$10^{-2}$ S cm$^{-1}$ ($8.3–9.7 \times 10^{-3}$ S cm$^{-1}$) at 95 °C (368 K) under mild humidity (RH 75%) [54]. Furthermore, the introduction of a lanthanide ion ($Eu^{3+}$) attracting water molecules led to robust composites exhibiting ultrahigh conductivities of $1.0–1.2 \times 10^{-2}$ S cm$^{-1}$ at 95 °C (368 K) under humidity (RH 90%) [55]. The combination of a Eu-introduced Preyssler-type POM with poly(vinyl alcohol) (PVA) realized a high proton conductivity of $8.3 \times 10^{-3}$ S cm$^{-1}$ at 95 °C (368 K) under mild humidity (RH 75%) [56]. Polar Preyssler-type POMs of $[Ca(H_2O)P_5W_{30}O_{110}]^{13-}$ ($CaP_5W_{30}$) and $[Eu(H_2O)P_5W_{30}O_{110}]^{12-}$ ($EuP_5W_{30}$) formed a staggered array in the crystalline lattice, which surprisingly helped the emergence of ultrahigh proton conductivities of $2.8 \times 10^{-2}$ S cm$^{-1}$ ($CaP_5W_{30}$ system) and $2.3 \times 10^{-2}$ S cm$^{-1}$ ($EuP_5W_{30}$ system) under the same conditions [57]. The combination of Preyssler-type POMs and a PAA matrix is quite promising for solid electrolytes with ultrahigh proton conductivity.

## 3. Organically Modified POM (org-POM) Polymers

Some inorganic POM anions can react with an organic moiety to form covalent bonds between the POM skeleton and the organic moiety, which leads to organically modified POMs (denoted as org-POMs hereafter). Typical examples are shown in Figure 4. The synthetic methodology of org-POMs has dramatically progressed in recent decades and has attracted widespread attention for the bottom-up construction of functional materials [59–70]. org-POMs are synthesized by utilizing the reaction between an organic reagent and oxygen atoms of the oxo or hydroxo moiety of a native POM, causing the organic groups to covalently bond to the oxygen atoms of the POM (Figure 4a). In other words, org-POMs are organic moiety-grafted POM anions. Several organic moieties such as polymerizable and/or coordinative groups can be introduced into the native POM skeleton. The introduced moiety can be sequentially extended by several organic reactions such as a click reaction (Figure 4b). The molecular structure of org-POMs can be unambiguously characterized by several spectroscopic methods. Single-crystal X-ray diffraction analysis is also applicable when suitable crystals can be obtained. The native POMs utilized for the synthesis of org-POMs are typically lacunary Keggin- and Dawson-type POMs holding unsaturated oxygens (Figure 4c, left). Vanadium-substituted Dawson-type POMs and Anderson-type POMs with relatively active oxygens in the oxo or hydroxo group (Figure 4c, center and right) are also employed. Detailed syntheses of org-POMs have been comprehensively reviewed [60,65,68].

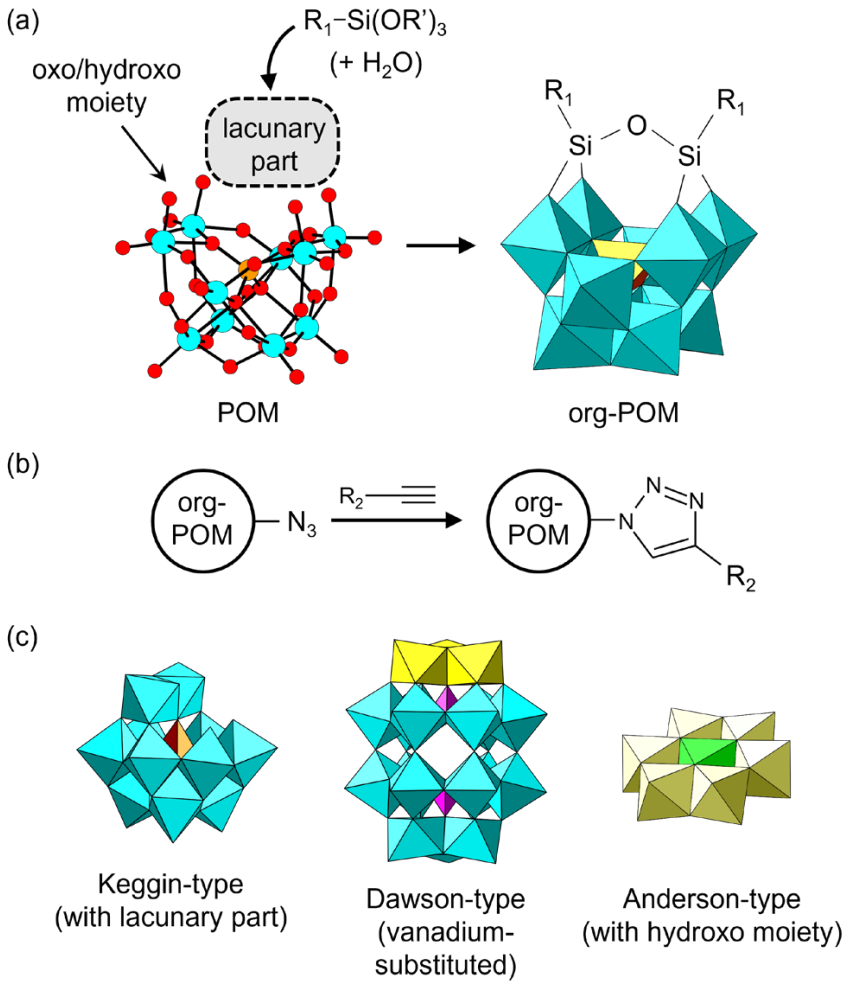



**Figure 4.** Organically modified POMs (org-POMs): (**a**) typical synthetic strategy for grafting an organic moiety to a POM anion; (**b**) typical extension method for grafted organic moieties; (**c**) examples of POM skeletons used for the synthesis of org-POMs.

Several org-POMs with a polymerizable moiety and their derivative polymers have been synthesized since 1992 [71–90]. These polymerizable org-POMs work as monomers, and POM–polymer composites with distinct compositions and structures have been obtained. Single crystals of polymerizable org-POMs have been reported as rare examples [74–76]. Moore et al. synthesized an org-POM with a styrylimido moiety by using a Lindqvist POM ($[Mo_6O_{19}]^{2-}$, $Mo_6$) (Figure 5a, org-$Mo_6$-V) [74]. The single crystals were obtained by diffusion of diethylether vapor into an acetonitrile solution as tetrabutylammonium (TBA) salt. This single-crystalline org-POM monomer was successfully copolymerized with 4-methylstyrene (MS) by radical polymerization using 2,2′-azobis(isobutyronitrile) (AIBN). Lu et al. reported org-$Mo_6$ derivatives with iodobenzene or ethynylbenzene moieties [75]. Single crystals of an ethynylbenzene-grafted org-POM were crystallized from the concentrated solution as TBA salt (Figure 5b, org-$Mo_6$-E). Org-$Mo_6$-E was polymerized with an iodobenzene derivative (ID) by the Sonogashira coupling reaction to obtain a π-electron-conjugated polymer. The conjugated polymers synthesized from Org-$Mo_6$-E were processed into thin films, and their application as organic photovoltaic cells was investigated. Similar conjugated polymers derived from single-crystalline org-$Mo_6$ can be prepared by a one-pot synthesis [76].

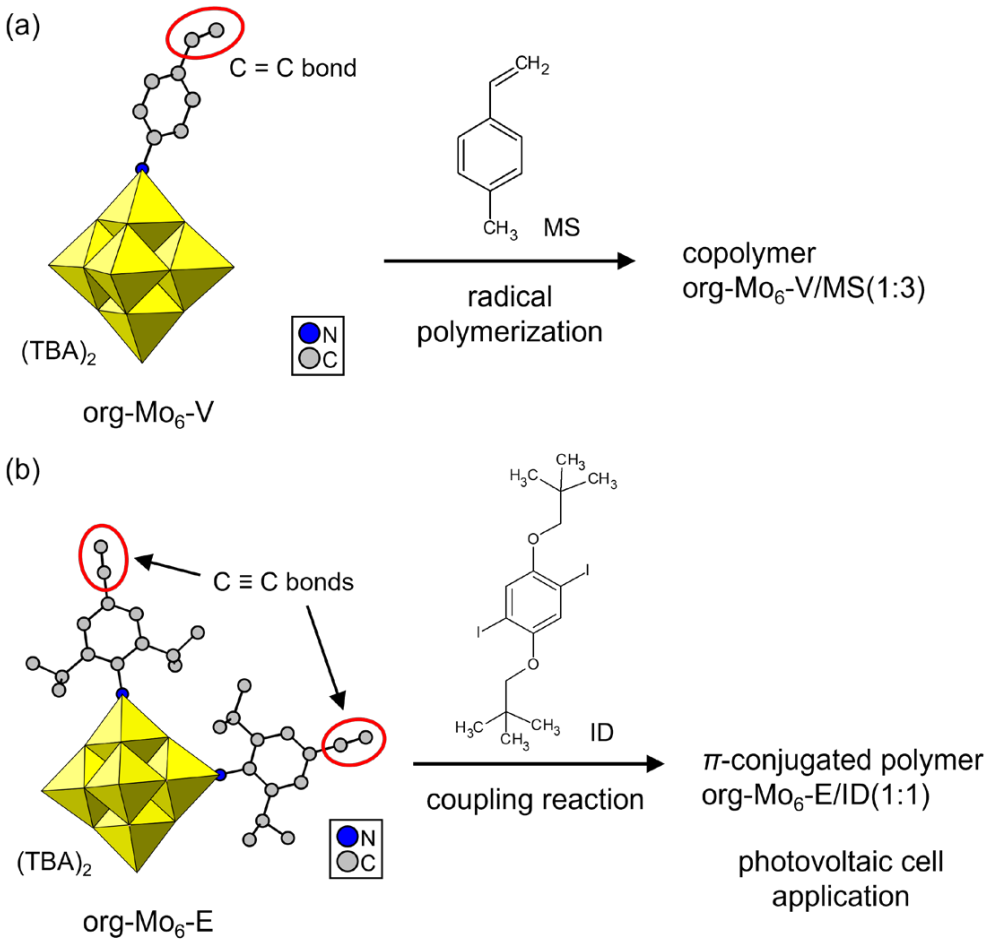



**Figure 5.** POM–polymer composites synthesized from single-crystalline polymerizable org-$Mo_6$ anions. Polymerizable groups are indicated by red ellipsoids. The org-POM/comonomer ratios in the copolymer are indicated in the figure: (**a**) org-$Mo_6$ with a styryl moiety (org-$Mo_6$-V); (**b**) org-$Mo_6$ with ethynylbenzene moieties (org-$Mo_6$-E).

Hasegawa and Nomiya et al. employed a mono-lacunary Dawson-type POM ([$\alpha_2$-$P_2W_{17}O_{61}$]$^{10-}$, $P_2W_{17}$) as a native skeleton to obtain org-POMs in dimethylammonium (DMA) salt forms [86–88]. Polymerizable POMs decorated with methacryloyl, acryloyl, and allyl moieties were grown as single crystals (Figure 6). In the case that organosilyl reagents were utilized, two organic moieties were introduced into one Dawson-type $P_2W_{17}$ skeleton (Figure 6a–c) [86–88], while one organic moiety was grafted onto one $P_2W_{17}$ skeleton when an organogermyl reagent was used (Figure 6d) [88]. This was due to the larger atomic size of germanium compared to silicon. Two organosilyl units can be replaced by forming a Si–O–Si bond in the lacunary space of one W atom, while only one organogermyl unit can enter the lacunary space. The DMA cation in an org-POM with a methacryloyl moiety (org-$PW_{17}$-MA, Figure 6a) was exchanged with a proton by using an ion-exchange resin [87]. The resulting acid form of org-$PW_{17}$-MA was utilized as a monomer to synthesize a copolymer with methyl methacrylate (MMA) by radical polymerization. The acidities of the acid-form org-$PW_{17}$-MA monomer and hybrid copolymer were evaluated using the Hammett indicators, demonstrating stronger acidity than 95% $H_2SO_4$. These acid-form org-$PW_{17}$-MA derivatives are promising for acid catalysts and proton-conducting materials.

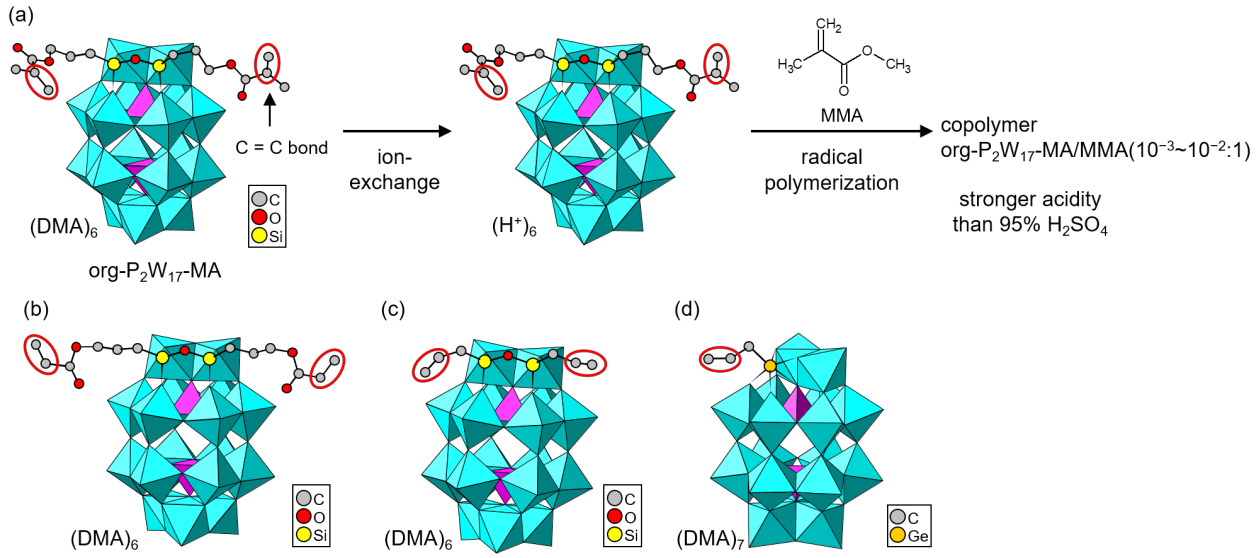



**Figure 6.** Single-crystalline org-POMs derived from a lacunary Dawson-type POM ($P_2W_{17}$). Polymerizable groups are indicated by red ellipsoids: (**a**) org-POM synthesized by an organosilyl reagent with a methacryloyl moiety (org-$P_2W_{17}$-MA) and POM–polymer composites. The org-$P_2W_{17}$-MA/comonomer ratio in the copolymer is indicated in the figure. (**b**) org-POM synthesized by an organosilyl reagent with an acryloyl moiety. (**c**) org-POM synthesized by an organosilyl reagent with an allyl moiety. (**d**) org-POM synthesized by an organogermyl reagent with an allyl moiety.

org-POM application to proton conductors is rather in its infancy [89–92]. Recently, the use of acid-type org-POMs obtained by the ion-exchange reaction as effective proton conductors has been verified [93–96]. Lu et al. reported the proton conductivity of org-POM polymers prepared from the TBA salt of a vanadium-substituted Dawson-type POM ($(TBA)_6H_3[P_2V_3W_{15}O_{62}]$, TBA-$P_2V_3W_{15}$) (Figure 7) [93,94]. The norbornene moiety was covalently bonded to the oxo groups of the substituted vanadium atoms (org-$P_2V_3W_{15}$) as a starting material. The TBA salt of org-$P_2V_3W_{15}$ was thoroughly characterized, but the single crystals were not obtained, probably due to the steric hindrance of the rather large organic moiety [35]. The org-POM monomer (TBA salt) was successfully polymerized by ring-opening metathesis polymerization. The obtained homopolymer could be copolymerized with norbornene-poly(ethylene oxide) (PEO) derivatives. The TBA cations of the homo- and copolymers were exchanged with protons by an ion-exchange resin, and their proton conductivities were investigated. The prepared copolymers exhibited ultrahigh proton conductivities of $1.11 \times 10^{-1}$ S cm$^{-1}$ for a random copolymer and $3.00–3.57 \times 10^{-2}$ S cm$^{-1}$ for a block copolymer under humidified conditions (RH 100%) at 80 °C (353 K) [94].

He et al. synthesized an org-POM functionalized by a PEG moiety which enhanced the proton conductivity of Nafion® [95]. A mono-lacunary Keggin-type POM ($K_8[SiW_{11}O_{39}]$, K-$SiW_{11}$) was employed in potassium ($K^+$) salt form as a native skeleton, and two PEG branches were introduced by using an organosilyl reagent, which resulted in the $K^+$ salt of amphiphilic org-$SiW_{11}$ (Figure 8). Two long PEG moieties might prevent the growth of single crystals [35,97]. The $K^+$ cation of org-$SiW_{11}$ was exchanged with a proton by an ion-exchange resin. Amphiphilic org-$SiW_{11}$ in $H^+$ form had high miscibility with Nafion®, and was co-assembled to prepare hybrid thin films. Supramolecular interactions between the amphiphilic org-$SiW_{11}$ and Nafion® led to stable immobilization of the POM in Nafion®. The proton conductivity of the amphiphilic org-$SiW_{11}$ (3 wt %)-added Nafion® reached an ultrahigh value of $2.26 \times 10^{-1}$ S cm$^{-1}$ under humidified conditions (RH 100%) at 80 °C (353 K). The org-$SiW_{11}$-added Nafion® showed additional enhancements in tensile strength (12.6 MPa) and fuel cell performance (power density 372 mW cm$^{-2}$, maximum current density 1.15 A cm$^{-2}$), which were both superior to those of pristine Nafion®. Fluoroalkyl-

functionalized org-$SiW_{11}$ was further demonstrated to be a supramolecular additive for Nafion® by the same group [96]. The proton conductivity and proton/vanadium selectivity were improved compared to pristine Nafion®, being applicable to fuel cells and vanadium flow batteries.

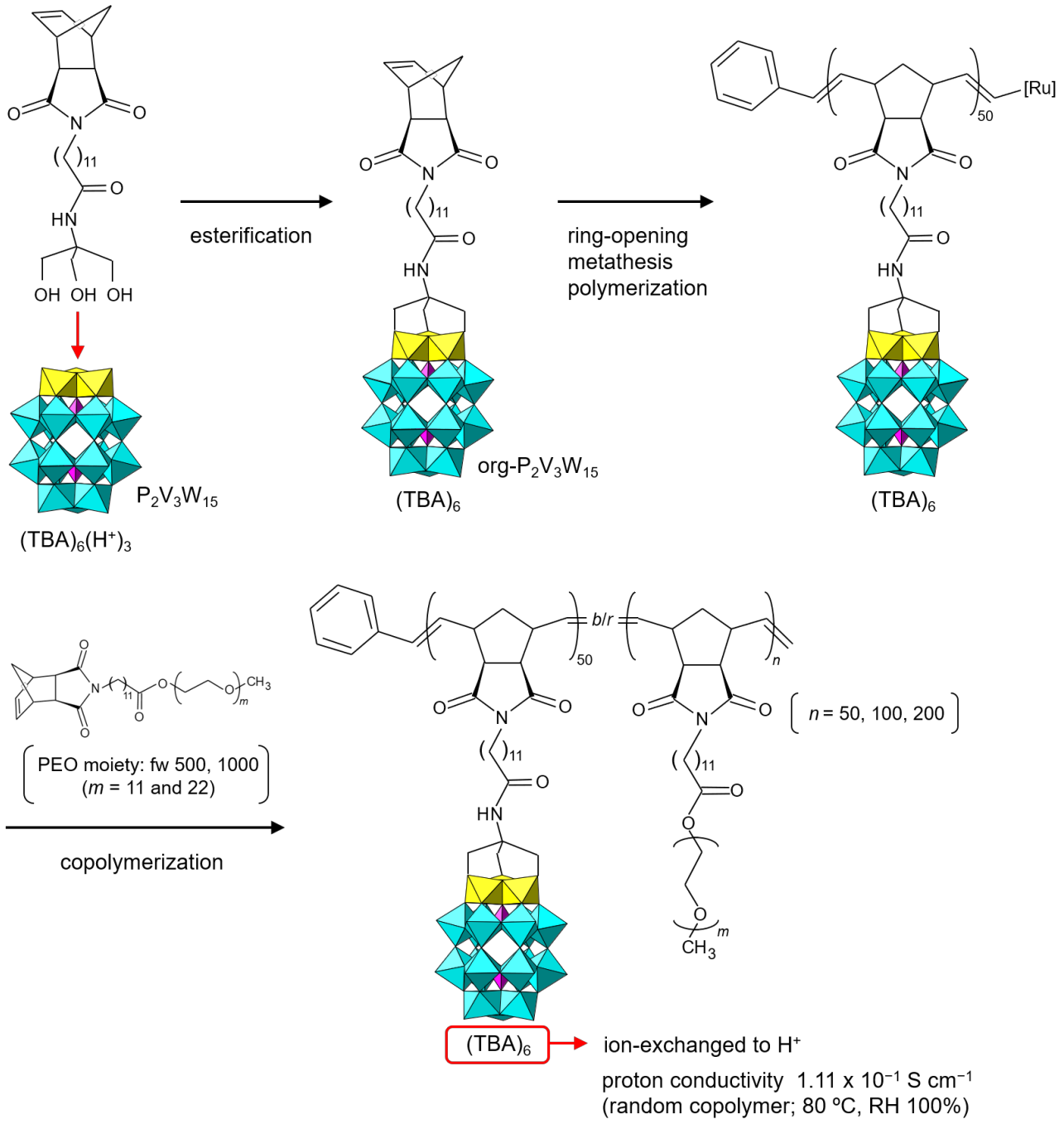



**Figure 7.** Synthetic procedure of org-$P_2V_3W_{15}$ anion and proton-conductive POM–polymer composite. The proton conductivity of the POM–polymer composite is indicated.

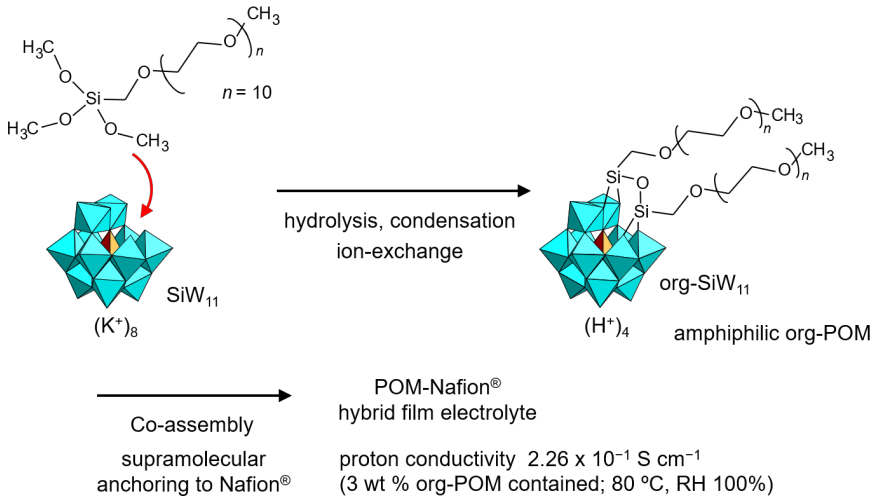



**Figure 8.** Synthetic procedure of amphiphilic org-$SiW_{11}$ anion and proton-conductive POM–polymer composites. The proton conductivity of the POM–polymer composite is indicated.

## 4. POM Hybrid Polymers Utilizing Polymerizable Cations

The counter cation of POM compounds can be changed to control the physicochemical properties, such as the thermal stability and miscibility to hydrophilic or hydrophobic solvents [22–24]. Functional counter cations expand the possibilities of POM compounds. Introducing a polymerizable moiety into the counter cations of POM anions will lead to the preparation of another class of POM–polymer composites. Li et al. synthesized a polymerizable surfactant, dodecyl(11-methacryloyloxyundecyl)dimethylammonium (DMDA), and used it to wrap an emissive europium-containing POM ($[EuW_{10}O_{36}]^{9-}$, $EuW_{10}$) (Figure 9) [98]. The amphiphilic DMDA-wrapped $EuW_{10}$ was soluble in conventional organic solvents and reacted with methyl methacrylate (MMA) by radical polymerization. The obtained copolymer of DMDA-wrapped $EuW_{10}$ and MMA was an excellently transparent polymer composite, exhibiting characteristic emission derived from $EuW_{10}$. The emission properties were retained after polymerization reactions.

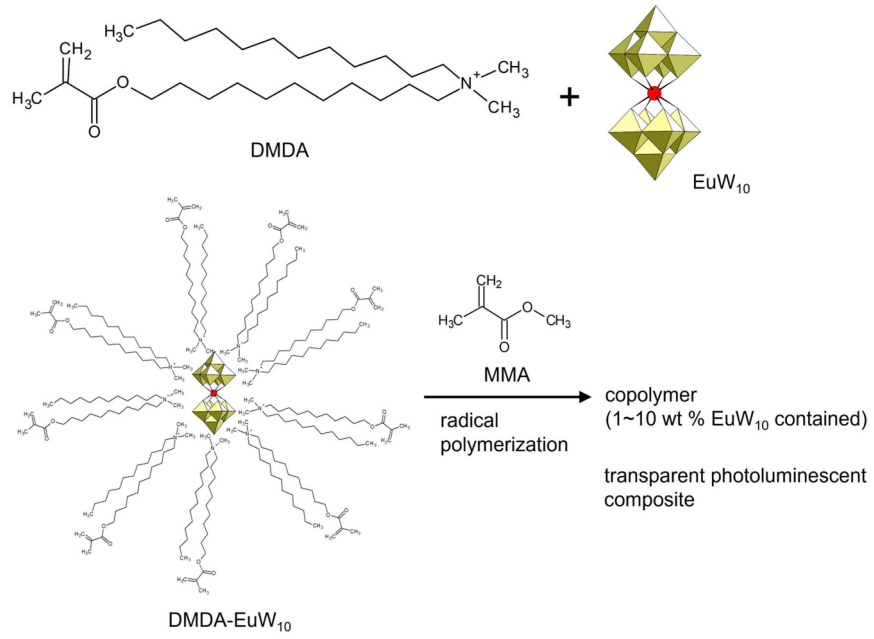



**Figure 9.** Synthetic procedure of inorganic–organic hybrid monomer and polymer utilizing photoluminescent $EuW_{10}$ and polymerizable DMDA cation. The DMDA-$EuW_{10}$/MMA ratio in the copolymer is indicated in the figure.

To explore the possibilities of POMs with polymerizable cations as solid electrolytes, we designed polymerizable ionic liquid cations (Figure 10a) [99–104]. The cations consist of imidazolium ionic liquid decorated with a methacryloyl group (denoted as MAIm). The ionic liquid contributes to the emergence of conductivity [15,16], and the properties of MAIm can be controlled by changing the substituent of the imidazolium moiety. MAIm with a methyl group ($MAImC_1$) can be hybridized with Keggin-type POMs ($PW_{12}$ and $SiW_{12}$) to obtain single crystals of hybrid monomers ($MAImC_1$-$PW_{12}$ and $MAImC_1$-$SiW_{12}$) (Figure 11). $MAImC_1$-$PW_{12}$ and $MAImC_1$-$SiW_{12}$ are polymerizable by radical polymerization, resulting in hybrid homopolymers [99,100]. Additionally, $MAImC_1$-$PW_{12}$ and $MAImC_1$-$SiW_{12}$ can be polymerized with butyl methacrylate (BMA) and a polymerizable ionic liquid with a long alkyl chain ($MAImC_8$-Br). Copolymerization with $MAImC_8$-Br enhanced the proton conductivity with humidity (RH 95%) at 40 °C (313 K), reaching $5.7 \times 10^{-4}$ S cm$^{-1}$ for $MAImC_1$-$PW_{12}$ and $2.7 \times 10^{-3}$ S cm$^{-1}$ for $MAImC_1$-$SiW_{12}$ (Figure 11).

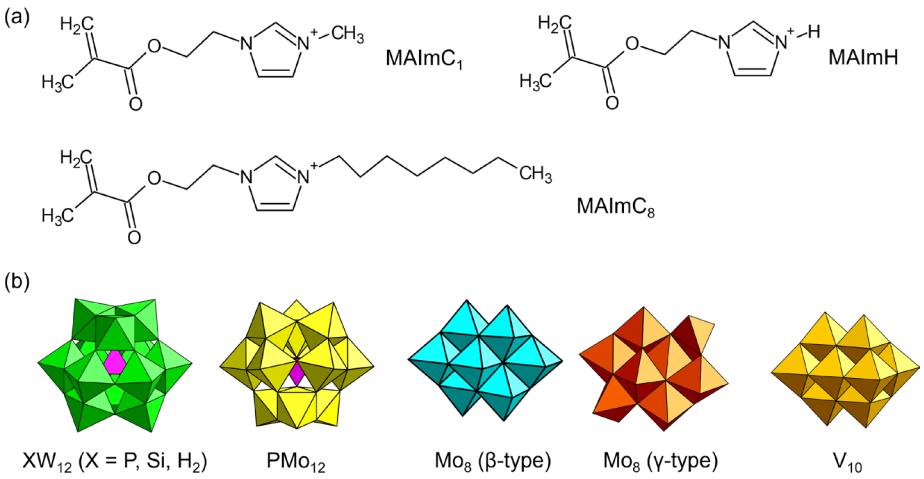



**Figure 10.** Molecular structures of (**a**) polymerizable ionic liquids, and (**b**) POM anions crystallized with polymerizable ionic liquids.

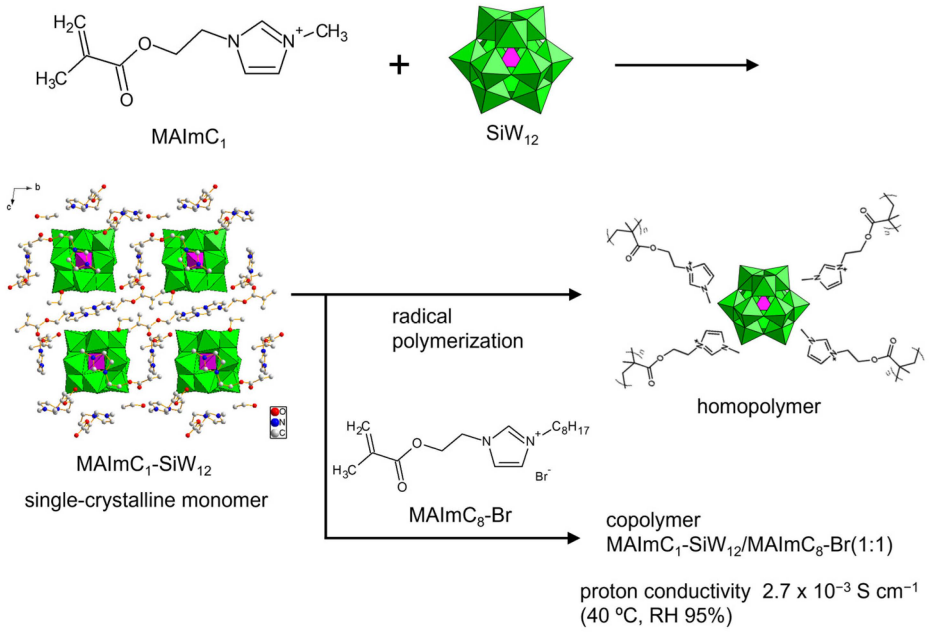



**Figure 11.** Synthetic procedure of single-crystalline monomer and proton-conductive hybrid polymers utilizing polymerizable $MAImC_1$ cation and $SiW_{12}$.

The polymerizable $MAImC_1$ cation can be crystallized with other Keggin-type POMs ($[H_2W_{12}O_{40}]^{6-}$ ($H_2W_{12}$) and $[PMo_{12}O_{40}]^{3-}$ ($PMo_{12}$)) with different negative charges or constituent atoms [101]. In both hybrid crystals, all counter cations were replaced by $MAImC_1$ located in the vicinity of $H_2W_{12}$ and $PMo_{12}$, which may have caused charge transfer under photoexcitation. The yellow-green $MAImC_1$-$PMo_{12}$ crystal contained a small amount of dark blue-colored reduced species in most non-reduced yellow $PMo_{12}$ anions, indicating a weak charge-transfer salt.

The $MAImC_1$ cation formed single crystals with isopolyoxometalates such as $[Mo_8O_{26}]^{4-}$ ($Mo_8$) and $[V_{10}O_{28}]^{6-}$ ($V_{10}$) accompanied by several metal cations. The hybrid crystal of $Mo_8$ was revealed to contain $Na^+$ to form $MAImC_1$-Na-$Mo_8$ as a polymerizable monomer [102]. The introduction of monovalent metal cations into POM–organic crystals has been reported [105,106]. The $Na^+$ cation can be exchanged with $Ag^+$ and $K^+$ to obtain $MAImC_1$-Ag-$Mo_8$ and $MAImC_1$-K-$Mo_8$. $MAImC_1$-Na-$Mo_8$ was polymerized by the radical polymerization reaction, and its conductivity with humidity (RH 95%) at 90 °C (363 K) was $5.1 \times 10^{-5}$ S cm$^{-1}$. As for the $V_{10}$ anion, single crystals with $MAImC_1$ were obtained solely under the coexistence of $Ca^{2+}$ and $Mg^{2+}$ as compounds of $MAImC_1$-Ca-$V_{10}$ and $MAImC_1$-Mg-$V_{10}$ (Figure 12) [103]. The reason that $MAImC_1$-Ca-$V_{10}$ and $MAImC_1$-Mg-$V_{10}$ were selectively obtained was not clear, but the introduction of divalent cations into POM–organic hybrid crystals is rare. The proton conductivities with humidity (RH 95%) at 80 °C (353 K) were a moderate value of $3.0 \times 10^{-4}$ S cm$^{-1}$ for $MAImC_1$-Ca-$V_{10}$ and a high value of $3.3 \times 10^{-3}$ S cm$^{-1}$ for $MAImC_1$-Mg-$V_{10}$. Such metal-cation-containing materials are promising for ionic conductors.

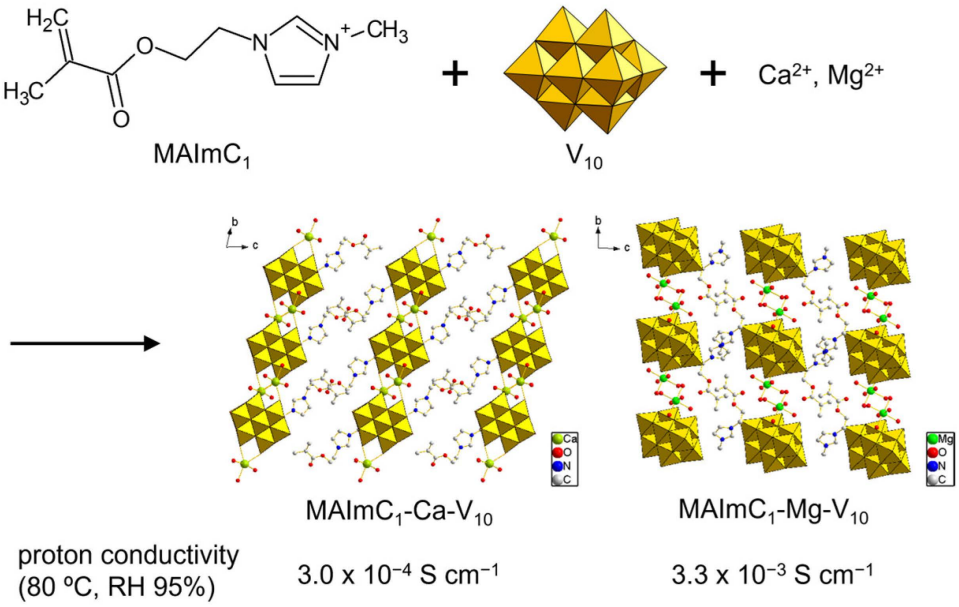



**Figure 12.** Proton-conductive hybrid crystals synthesized by using polymerizable $MAImC_1$ cation and $V_{10}$.

In MAIm cations, imidazolium substitutents can be designed. A deprotonatable MAImH cation was derived from MAIm without a methyl group. Amphiphilic $MAImC_8$ was obtained by introducing an octyl chain. Crystallization of POMs with these MAImH and $MAImC_8$ cations was reported to be rather difficult, but $Mo_8$ and $SiW_{12}$ were successfully crystallized [104]. Hybrid crystals with MAImH (MAImH-$Mo_8$ and MAImH-$SiW_{12}$) contain dissociative protons, which could be beneficial to proton conductivity. $MAImC_8$ hybrid crystals ($MAImC_8$-$Mo_8$ and $MAImC_8$-$SiW_{12}$) exhibited anisotropic layered or tunneling packing of POM anions in the crystal lattice derived from van der Waals interactions

of the alkyl chain (Figure 13). Such anisotropic POM packing would be effective for the emergence of conductivity.

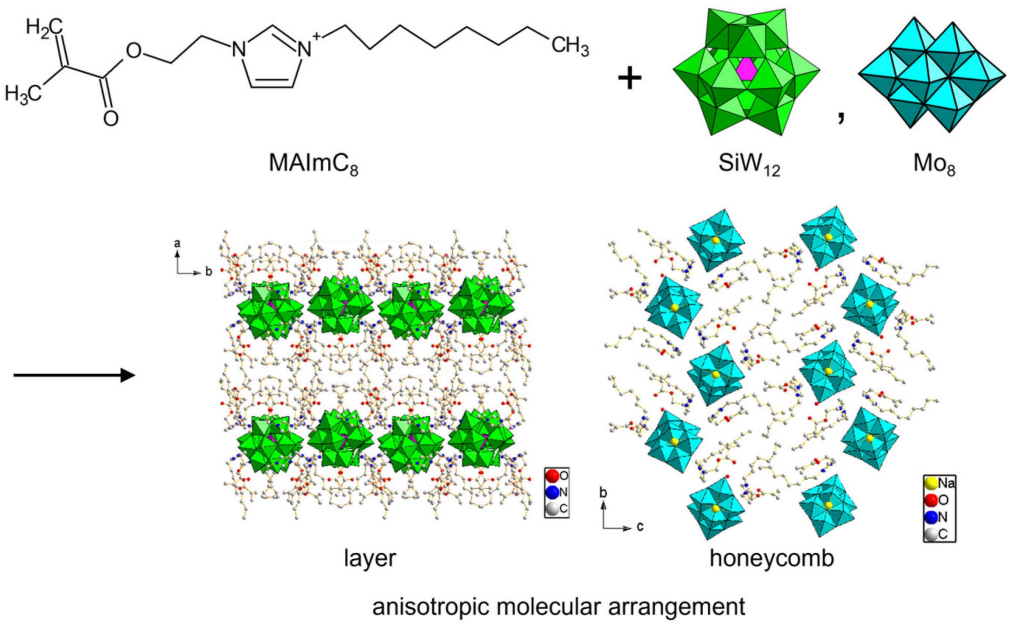



**Figure 13.** Inorganic–organic hybrid crystals of POMs derived from polymerizable $MAImC_8$ cation with amphiphilic moiety.

## 5. Summary and Outlook

Polyoxometalate–polymer (POM–polymer) composites with distinct compositions and structures have recently been synthesized as single-crystalline forms or by utilizing single-crystalline starting materials. These materials exhibit promising high proton conductivities of $10^{-3}$–$10^{-1}$ S cm$^{-1}$ as high-performance solid electrolytes for fuel cell batteries. Such POM–polymer composites can be categorized into three classes. Firstly, single-crystalline POM–polymer composites have been synthesized by combining POM compounds and polymer matrices such as polyethylene glycol (PEG) or polyallylamine (PAA). These POM–polymer composites have been obtained as single crystals. Secondly, organically modified POMs (org-POMs) have been employed as inorganic–organic hybrid monomers. Organic synthesis methods enable the flexible and precise design of org-POM monomers at a molecular level, which leads to the creation of various types of POM–polymer composites. Finally, inorganic–organic hybrid monomers consisting of POMs and polymerizable cations have been obtained as single crystals and utilized to prepare POM–polymer composites.

These POM–polymer composites can be obtained as single crystals. This is a great advantage when designing and controlling a material's composition, structure, and properties. However, the examples have been rare series of materials. Such POM–polymer composites hold flexible polymer matrices or long alkyl chains, which makes it difficult to obtain and analyze single crystals [35]. For POM–polymer composites using POMs without organic modification, the types of POM anion and counter cation can generally be selected, while POM–polymer composites utilizing org-POMs can be tailored in terms of their organic moiety. org-POM systems are quite promising and widely applied to many systems, from electrochemical to biological usage [59–70,107–111]. The native POM skeletons for org-POMs are rather limited, but the variety of POM skeletons is expanding. The search for appropriate combinations of POMs and organic components should be explored to obtain single crystals. A simpler and more effective methodology needs to be discovered in the future.

The POM–polymer composites overviewed here are under development; however, they are promising materials for the application of solid electrolytes for fuel cells. The relationship between the proton conductivity and material structures should be clarified to produce functional materials. The POM–polymer composites mentioned above are promising materials since they possess distinct compositions and structures at a molecular level. The proton conductivity of POM–polymer composites can be clearly associated with the material composition and structure. The revealed results can be effectively fed back to the development of synthetic strategies and to the molecular design of components for POM–polymer composites. The values of proton conductivity are now close to practical use for the solid electrolytes of fuel cell batteries. The next strategy for these POM–polymer composites will be to improve their durability in the presence of moisture and temperature and to investigate material processability.

**Funding:** This research was funded in part by JSPS KAKENHI (grant number JP21K05232), Research and Study Project of Tokai University Research Organization, and Izumi Science and Technology Foundation.

**Acknowledgments:** The author acknowledges the following researchers of Tokai University for their kind collaboration: Shinichi Koguchi, Kaito Sasaki, Masashi Higuchi, Yosuke Okamura, Naoki Shinyashiki, and Yu Nagase.

**Conflicts of Interest:** The author declares no conflicts of interest. The funders had no role in the design of the study; in the collection, analyses, or interpretation of data; in the writing of the manuscript; or in the decision to publish the results.

## References

1. Whittingham, M.S. Lithium batteries and cathode materials. *Chem. Rev.* **2004**, *104*, 4271–4301. [CrossRef] [PubMed]
2. Goodenough, J.B.; Park, K.-S. The Li-ion rechargeable battery: A perspective. *J. Am. Chem. Soc.* **2013**, *135*, 1167–1176. [CrossRef]
3. Yabuuchi, N.; Kubota, K.; Dahbi, M.; Komaba, S. Research development on sodium-ion batteries. *Chem. Rev.* **2014**, *114*, 11636–11682. [CrossRef]
4. Kundu, D.; Talaie, E.; Duffort, V.; Nazar, L.F. The emerging chemistry of sodium ion batteries for electrochemical energy storage. *Angew. Chem. Int. Ed.* **2015**, *54*, 3431–3448. [CrossRef]
5. Steele, B.C.H.; Heinzel, A. Materials for fuel-cell technologies. *Nature* **2001**, *414*, 345–352. [CrossRef] [PubMed]
6. Horike, S.; Umeyama, D.; Kitagawa, S. Ion conductivity and transport by porous coordination polymers and metal-organic frameworks. *Acc. Chem. Res.* **2013**, *46*, 2376–2384. [CrossRef]
7. Yoon, M.; Suh, K.; Natarajan, S.; Kim, K. Proton conduction in metal-organic frameworks and related modularly built porous solids. *Angew. Chem. Int. Ed.* **2013**, *52*, 2688–2700. [CrossRef]
8. Ramaswamy, P.; Wong, N.E.; Shimizu, G.K.H. MOFs as proton conductors-challenges and opportunities. *Chem. Soc. Rev.* **2014**, *43*, 5913–5932. [CrossRef] [PubMed]
9. Sadakiyo, M.; Yamada, T.; Kitagawa, H. Hydrated proton-conductive metal-organic frameworks. *ChemPlusChem* **2016**, *81*, 691–701. [CrossRef]
10. Kreuer, K.-D.; Paddison, S.J.; Spohr, E.; Schuster, M. Transport in proton conductors for fuel-cell applications: Simulations, elementary reactions, and phenomenology. *Chem. Rev.* **2004**, *104*, 4637–4678. [CrossRef]
11. Zhang, H.; Shen, P.K. Recent development of polymer electrolyte membranes for fuel cells. *Chem. Rev.* **2012**, *112*, 2780–2832. [PubMed]
12. Li, Q.; He, R.; Jensen, J.O.; Bjerrum, N.J. Approaches and recent development of polymer electrolyte membranes for fuel cells operating above 100 °C. *Chem. Mater.* **2003**, *15*, 4896–4915. [CrossRef]
13. Çelik, S.Ü.; Bozkurt, A.; Hosseini, S.S. Alternatives toward proton conductive anhydrous membranes for fuel cells: Heterocyclic protogenic solvents comprising polymer electrolytes. *Prog. Polym. Sci.* **2012**, *37*, 1265–1291. [CrossRef]
14. Chandan, A.; Hattenberger, M.; El-kharouf, A.; Du, S.; Dhir, A.; Self, V.; Pollet, B.G.; Ingram, A.; Bujalski, W. High temperature (HT) polymer electrolyte membrane fuel cells (PEMFC)—A review. *J. Power Sources* **2013**, *231*, 264–278. [CrossRef]
15. Watanabe, M.; Thomas, M.L.; Zhang, S.; Ueno, K.; Yasuda, T.; Dokko, K. Application of ionic liquids to energy storage and conversion materials and devices. *Chem. Rev.* **2017**, *117*, 7190–7239. [CrossRef]
16. Qian, W.; Texter, J.; Yan, F. Frontiers in poly(ionic liquid)s: Syntheses and applications. *Chem. Soc. Rev.* **2017**, *46*, 1124–1159. [CrossRef]

17. Qu, E.; Hao, X.; Xiao, M.; Han, D.; Huang, S.; Huang, Z.; Wang, S.; Meng, Y. Proton exchange membranes for high temperature proton exchange membrane fuel cells: Challenges and perspectives. *J. Power Sources* **2022**, *533*, 231386. [CrossRef]
18. Coronado, E.; Gómez-García, C.J. Polyoxometalate-based molecular materials. *Chem. Rev.* **1998**, *98*, 273–296. [CrossRef]
19. Long, D.-L.; Tsunashima, R.; Cronin, L. Polyoxometalates: Building blocks for functional nanoscale systems. *Angew. Chem. Int. Ed.* **2010**, *49*, 1736–1758. [CrossRef]
20. Sadakane, M.; Steckhan, E. Electrochemical properties of polyoxometalates as electrocatalysts. *Chem. Rev.* **1998**, *98*, 219–237. [CrossRef]
21. Gumerova, N.I.; Rompel, A. Synthesis, structures and applications of electron-rich polyoxometalates. *Nat. Rev. Chem.* **2018**, *2*, 0112. [CrossRef]
22. Okuhara, T.; Mizuno, N.; Misono, M. Catalytic chemistry of heteropoly compounds. *Adv. Catal.* **1996**, *41*, 113–252.
23. Misra, A.; Kozma, K.; Streb, C.; Nyman, M. Beyond charge balance: Counter-cations in polyoxometalate chemistry. *Angew. Chem. Int. Ed.* **2020**, *59*, 596–612. [CrossRef] [PubMed]
24. Ogiwara, N.; Iwano, T.; Ito, T.; Uchida, S. Proton conduction in ionic crystals based on polyoxometalates. *Coord. Chem. Rev.* **2022**, *462*, 214524. [CrossRef]
25. Nakamura, O.; Kodama, T.; Ogino, I.; Miyake, Y. High-conductivity solid proton conductors: Dodecamolybdophosphoric acid and dodecatungstophosphoric acid crystals. *Chem. Lett.* **1979**, *8*, 17–18. [CrossRef]
26. Mioč, U.B.; Todorović, M.R.; Davidović, M.; Colomban, P.; Holclajtner-Antunović, I. Heteropoly compounds-From proton conductors to biomedical agents. *Solid State Ionics* **2005**, *176*, 3005–3017. [CrossRef]
27. Bourlinos, A.B.; Raman, K.; Herrera, R.; Zhang, Q.; Archer, L.A.; Giannelis, E.P. A liquid derivative of 12-tungstophosphoric acid with unusually high conductivity. *J. Am. Chem. Soc.* **2004**, *126*, 15358–15359. [CrossRef] [PubMed]
28. Kukino, T.; Kikuchi, R.; Takeguchi, T.; Matsui, T.; Eguchi, K. Proton conductivity and stability of $Cs_2HPW_{12}O_{40}$ electrolyte at intermediate temperatures. *Solid State Ionics* **2005**, *176*, 1845–1848. [CrossRef]
29. Wu, X.; Tong, X.; Wu, Q.; Ding, H.; Yan, W. Reversible phase transformation-type electrolyte based on layered shape polyoxometalate. *J. Mater. Chem. A* **2014**, *2*, 5780–5784. [CrossRef]
30. Ma, H.; Liu, B.; Li, B.; Zhang, L.; Li, Y.-G.; Tan, H.-Q.; Zang, H.-Y.; Zhu, G. Cationic covalent organic frameworks: A simple platform of anionic exchange for porosity tuning and proton conduction. *J. Am. Chem. Soc.* **2016**, *138*, 5897–5903. [CrossRef]
31. Liu, J.-C.; Han, Q.; Chen, L.-J.; Zhao, J.-W.; Streb, C.; Song, Y.-F. Aggregation of giant cerium-bismuth tungstate clusters into a 3D porous framework with high proton conductivity. *Angew. Chem. Int. Ed.* **2018**, *57*, 8416–8420. [CrossRef] [PubMed]
32. Yang, P.; Alsufyani, M.; Emwas, A.-H.; Chen, C.; Khashab, N.M. Lewis acid guests in a $\{P_8W_{48}\}$ archetypal polyoxotungstate host: Enhanced proton conductivity via metal-oxo cluster within cluster assemblies. *Angew. Chem. Int. Ed.* **2018**, *57*, 13046–13051. [CrossRef]
33. Li, Z.; Lin, L.-D.; Yu, H.; Li, X.-X.; Zheng, S.-T. All-inorganic ionic porous material based on giant spherical polyoxometalates containing core-shell $K_6$@$K_{36}$-water cage. *Angew. Chem. Int. Ed.* **2018**, *57*, 15777–15781. [CrossRef] [PubMed]
34. Sun, X.; Liu, S.; Zhang, S.; Dang, T.; Tian, H.; Lu, Y.; Liu, S. High proton conductivity achieved by the self-assembly of POM-based acid-base adduct in SBA-15 over a wide range from −40 to 85 °C. *ACS Appl. Energy Mater.* **2020**, *3*, 1242–1248. [CrossRef]
35. Ito, T. Inorganic-organic hybrid surfactant crystals: Structural aspects and functions. *Crystals* **2016**, *6*, 24. [CrossRef]
36. Taira, M.; Sato, H.; Fukumoto, K.; Misawa, T.; Naruke, H.; Ito, T. Polyoxovanadate-surfactant hybrid layered crystals toward anhydrous proton conductors. *J. Mol. Struct.* **2021**, *1226*, 129355. [CrossRef]
37. Asensio, J.A.; Sánchez, E.M.; Gómez-Romero, P. Proton-conducting membranes based on benzimidazole polymers for high-temperature PEM fuel cells. A chemical quest. *Chem. Soc. Rev.* **2010**, *39*, 3210–3239. [CrossRef]
38. Herring, A.M. Inorganic-polymer composite membranes for proton exchange membrane fuel cells. *J. Macromol. Sci. Part C* **2006**, *46*, 245–296. [CrossRef]
39. Honma, I.; Yamada, M. Bio-inspired membranes for advanced polymer electrolyte fuel cells. Anhydrous proton-conducting membrane via molecular self-assembly. *Bull. Chem. Soc. Jpn.* **2007**, *80*, 2110–2123. [CrossRef]
40. Qi, W.; Wu, L. Polyoxometalate/polymer hybrid materials: Fabrication and properties. *Polym. Int.* **2009**, *58*, 1217–1225. [CrossRef]
41. Kourasi, M.; Wills, R.G.A.; Shah, A.A.; Walsh, F.C. Heteropolyacids for fuel cell applications. *Electrochim. Acta* **2014**, *127*, 454–466. [CrossRef]
42. Herrmann, S.; Ritchie, C.; Streb, C. Polyoxometalate-conductive polymer composites for energy conversion, energy storage and nanostructured sensors. *Dalton Trans.* **2015**, *44*, 7092–7104. [CrossRef]
43. Jiao, K.; Xuan, J.; Du, Q.; Bao, Z.; Xie, B.; Wang, B.; Zhao, Y.; Fan, L.; Wang, H.; Hou, Z.; et al. Designing the next generation of proton-exchange membrane fuel cells. *Nature* **2021**, *595*, 361–369. [CrossRef] [PubMed]
44. Yamada, M.; Honma, I. Heteropolyacid-encapsulated self-assembled materials for anhydrous proton-conducting electrolytes. *J. Phys. Chem. B* **2006**, *110*, 20486–20490. [CrossRef] [PubMed]

45. Oh, S.-Y.; Yoshida, T.; Kawamura, G.; Muto, H.; Sakai, M.; Matsuda, A. Inorganic-organic composite electrolytes consisting of polybenzimidazole and Cs-substituted heteropoly acids and their application for medium temperature fuel cells. *J. Mater. Chem.* **2010**, *20*, 6359–6366. [CrossRef]
46. Lu, S.; Xu, X.; Zhang, J.; Peng, S.; Liang, D.; Wang, H.; Xiang, Y. A Self-Anchored Phosphotungstic Acid Hybrid Proton Exchange Membrane Achieved via One-Step Synthesis. *Adv. Energy Mater.* **2014**, *4*, 1400842. [CrossRef]
47. Zheng, Z.; Li, M.; Zhou, Q.; Cai, L.; Yin, J.-F.; Cao, Y.; Yin, P. Polyoxometalate-poly(ethylene oxide) nanocomposites for flexible anhydrous solid-state proton conductors. *ACS Appl. Nano Mater.* **2021**, *4*, 811–819. [CrossRef]
48. Zhang, L.; Cui, T.; Cao, X.; Zhao, C.; Chen, Q.; Wu, L.; Li, H. Inorganic-macroion-induced formation of bicontinuous block copolymer nanocomposites with enhanced conductivity and modulus. *Angew. Chem. Int. Ed.* **2017**, *56*, 9013–9017. [CrossRef]
49. Inoue, T.; Uma, T.; Nogami, M. Performance of $H_2/O_2$ fuel cell using membrane electrolyte of phosphotungstic acid-modified 3-glycidoxypropyl-trimethoxysilanes. *J. Membrane Sci.* **2008**, *323*, 148–152. [CrossRef]
50. Lakshminarayana, G.; Nogami, M. Synthesis and characterization of proton conducting inorganic-organic hybrid nanocomposite membranes based on tetraethoxysilane/trimethylphosphate/3-glycidoxypropyltrimethoxysilane/heteropoly acids. *Electrochim. Acta* **2009**, *54*, 4731–4740. [CrossRef]
51. Tsuboi, M.; Hibino, M.; Mizuno, N.; Uchida, S. Crystalline polyoxometalate (POM)-polyethylene glycol (PEG) composites aimed as non-humidified intermediate-temperature proton conductors. *J. Solid State Chem.* **2016**, *234*, 9–14. [CrossRef]
52. Ogiwara, N.; Tomoda, M.; Miyazaki, S.; Wen, Z.; Takatsu, H.; Kageyama, H.; Misawa, T.; Ito, T.; Uchida, S. Integrating molecular design and crystal engineering approaches in non-humidified intermediate-temperature proton conductors based on a Dawson-type polyoxometalate and poly(ethylene glycol) derivatives. *Nanoscale* **2021**, *13*, 8049–8057. [CrossRef]
53. Niinomi, K.; Miyazawa, S.; Hibino, M.; Mizuno, N.; Uchida, S. High proton conduction in crystalline composites based on Preyssler-type polyoxometalates and polymers under nonhumidified or humidified conditions. *Inorg. Chem.* **2017**, *56*, 15187–15193. [CrossRef]
54. Iwano, T.; Miyazawa, S.; Osuga, R.; Kondo, J.N.; Honjo, K.; Kitao, T.; Uemura, T.; Uchida, S. Confinement of poly(allylamine) in Preyssler-type polyoxometalate and potassium ion framework for enhanced proton conductivity. *Commun. Chem.* **2019**, *2*, 9. [CrossRef]
55. Iwano, T.; Shitamatsu, T.; Ogiwara, N.; Okuno, M.; Kikukawa, Y.; Ikemoto, S.; Shirai, S.; Muratsugu, S.; Waddell, P.G.; Errington, R.J.; et al. Ultrahigh Proton Conduction via Extended hydrogen-bonding network in a Preyssler-type polyoxometalate-based framework functionalized with a lanthanide ion. *ACS Appl. Mater. Interfaces* **2021**, *13*, 19138–19147. [CrossRef] [PubMed]
56. Iwano, T.; Shirai, S.; Chen, C.; Weng, Z.; Kikukawa, Y.; Muratsugu, S.; Tada, M.; Takatsu, H.; Kageyama, H.; Uchida, S. Incorporation of poly(vinyl alcohol) into an inorganic framework based on Eu-bonded Preyssler-type phosphotungstate for enhanced proton conduction. *ACS Appl. Polym. Mater.* **2024**, *6*, 7926–7931. [CrossRef]
57. Iwano, T.; Akutsu, D.; Ubukata, H.; Ogiwara, N.; Kikukawa, Y.; Wang, S.; Yan, L.-K.; Kageyama, H.; Uchida, S. Tuning proton conduction by staggered arrays of polar Preyssler-type oxoclusters. *J. Am. Chem. Soc.* **2024**, *146*, 26113–26120. [CrossRef]
58. Buchecker, T.; Le Goff, X.; Naskar, B.; Pfitzner, A.; Diat, O.; Bauduin, P. Polyoxometalate/polyethylene glycol interactions in water: From nanoassemblies in water to crystal formation by electrostatic screening. *Chem. Eur. J.* **2017**, *23*, 8434–8442. [CrossRef]
59. Peng, Z. Rational synthesis of covalently bonded organic-inorganic hybrids. *Angew. Chem. Int. Ed.* **2004**, *43*, 930–935. [CrossRef]
60. Dolbecq, A.; Dumas, E.; Mayer, C.R.; Mialane, P. Hybrid organic-inorganic polyoxometalate compounds: From structural diversity to applications. *Chem. Rev.* **2010**, *110*, 6009–6048. [CrossRef]
61. Li, D.; Yin, P.; Liu, T. Supramolecular architectures assembled from amphiphilic hybrid polyoxometalates. *Dalton Trans.* **2012**, *41*, 2853–2861. [CrossRef]
62. Santoni, M.-P.; Hanan, G.S.; Hasenknopf, B. Covalent multi-component systems of polyoxometalates and metal complexes: Toward multi-functional organic–inorganic hybrids in molecular and material sciences. *Coord. Chem. Rev.* **2014**, *281*, 64–85. [CrossRef]
63. Carraro, M.; Gross, S. Hybrid materials based on the embedding of organically modified transition metal oxoclusters or polyoxometalates into polymers for functional applications: A Review. *Materials* **2014**, *7*, 3956–3989. [CrossRef] [PubMed]
64. Wu, H.; Yang, H.-K.; Wang, W. Covalently-linked polyoxometalate–polymer hybrids: Optimizing synthesis, appealing structures and prospective applications. *New J. Chem.* **2016**, *40*, 886–897. [CrossRef]
65. Kibler, A.J.; Newton, G.N. Tuning the electronic structure of organic-inorganic hybrid polyoxometalates: The crucial role of the covalent linkage. *Polyhedron* **2018**, *154*, 1–20. [CrossRef]
66. Yan, J.; Zheng, X.; Yao, J.; Xu, P.; Miao, Z.; Li, J.; Lv, Z.; Zhang, Q.; Yan, Y. Metallopolymers from organically modified polyoxometalates (MOMPs): A review. *J. Organomet. Chem.* **2019**, *884*, 1–16. [CrossRef]
67. Zhai, L.; Li, H. Polyoxometalate-polymer hybrid materials as proton exchange membranes for fuel cell applications. *Molecules* **2019**, *24*, 3425. [CrossRef] [PubMed]
68. Anyushin, A.V.; Kondinski, A.; Parac-Vogt, T.N. Hybrid polyoxometalates as post-functionalization platforms: From fundamentals to emerging applications. *Chem. Soc. Rev.* **2020**, *49*, 382–432. [CrossRef]

69. Cameron, J.M.; Guillemot, G.; Galambos, T.; Amin, S.S.; Hampson, E.; Mall Haidaraly, K.; Newton, G.N.; Izzet, G. Supramolecular assemblies of organo-functionalised hybrid polyoxometalates: From functional building blocks to hierarchical nanomaterials. *Chem. Soc. Rev.* **2022**, *51*, 293–328. [CrossRef]
70. Wei, Z.; Wang, J.; Yu, H.; Han, S.; Wei, Y. Recent advances of Anderson-type polyoxometalates as catalysts largely for oxidative transformations of organic molecules. *Molecules* **2022**, *27*, 5212. [CrossRef]
71. Judeinstein, P. Synthesis and properties of polyoxometalates based inorganic-organic polymers. *Chem. Mater.* **1992**, *4*, 4–7. [CrossRef]
72. Mayer, C.R.; Thouvenot, R.; Lalot, T. New hybrid covalent networks based on polyoxometalates: Part 1. hybrid networks based on poly(ethylmethacrylate) chains covalently cross-linked by heteropolyanions: Synthesis and swelling properties. *Chem. Mater.* **2000**, *12*, 257–260. [CrossRef]
73. Mayer, C.R.; Thouvenot, R.; Lalot, T. Hybrid hydrogels obtained by the copolymerization of acrylamide with aggregates of methacryloyl derivatives of polyoxotungstates. A comparison with polyacrylamide hydrogels with trapped aggregates. *Macromolecules* **2000**, *33*, 4433–4437. [CrossRef]
74. Moore, A.R.; Kwen, H.; Beatty, A.M.; Maatta, E.A. Organoimido-polyoxometalates as polymer pendants. *Chem. Commun.* **2000**, 1793–1794. [CrossRef]
75. Lu, M.; Xie, B.; Kang, J.; Chen, F.-C.; Yang, Y.; Peng, Z. Synthesis of main-chain polyoxometalate-containing hybrid polymers and their applications in photovoltaic cells. *Chem. Mater.* **2005**, *17*, 402–408. [CrossRef]
76. Xu, B.; Lu, M.; Kang, J.; Wang, D.; Brown, J.; Peng, Z. Synthesis and optical properties of conjugated polymers containing polyoxometalate clusters as side-chain pendants. *Chem. Mater.* **2005**, *17*, 2841–2851. [CrossRef]
77. Hasenknopf, B.; Delmont, R.; Herson, P.; Gouzerh, P. Anderson-type heteropolymolybdates containing tris(alkoxo) ligands: Synthesis and Structural Characterization. *Eur. J. Inorg. Chem.* **2002**, *2002*, 1081–1087. [CrossRef]
78. Bareyt, S.; Piligkos, S.; Hasenknopf, B.; Gouzerh, P.; Lacôte, E.; Thorimbert, S.; Malacria, M. Highly efficient peptide bond formation to functionalized Wells-Dawson-type polyoxotungstates. *Angew. Chem. Int. Ed.* **2003**, *42*, 3404–3406. [CrossRef]
79. Zhang, J.; Song, Y.-F.; Cronin, L.; Liu, T. Self-assembly of organic-inorganic hybrid amphiphilic surfactants with large polyoxometalates as polar head groups. *J. Am. Chem. Soc.* **2008**, *130*, 14408–14409. [CrossRef]
80. Han, Y.; Xiao, Y.; Zhang, Z.; Liu, B.; Zheng, P.; He, S.; Wang, W. Synthesis of polyoxometalate-polymer hybrid polymers and their hybrid vesicular assembly. *Macromolecules* **2009**, *42*, 6543–6548. [CrossRef]
81. Miao, W.-K.; Yan, Y.-K.; Wang, X.-L.; Xiao, Y.; Ren, L.-J.; Zheng, P.; Wang, C.-H.; Ren, L.-X.; Wang, W. Incorporation of polyoxometalates into polymers to create linear poly(polyoxometalate)s with catalytic function. *ACS Macro Lett.* **2014**, *3*, 211–215. [CrossRef] [PubMed]
82. Tong, U.; Chen, W.; Ritchie, C.; Wang, X.; Song, Y.-F. Reversible light-driven polymerization of polyoxometalate tethered with coumarin molecules. *Chem. Eur. J.* **2014**, *20*, 1500–1504. [CrossRef]
83. Macdonell, A.; Johnson, N.A.B.; Surman, A.J.; Cronin, L. Configurable nanosized metal oxide oligomers via precise "click" coupling control of hybrid polyoxometalates. *J. Am. Chem. Soc.* **2015**, *137*, 5662–5665. [CrossRef] [PubMed]
84. Li, X.-X.; Wang, Y.-X.; Wang, R.-H.; Cui, C.-Y.; Tian, C.-B.; Yang, G.-Y. Designed assembly of heterometallic cluster organic frameworks based on Anderson-type polyoxometalate clusters. *Angew. Chem. Int. Ed.* **2016**, *55*, 6462–6466. [CrossRef] [PubMed]
85. Xu, W.; Pei, X.; Diercks, C.S.; Lyu, H.; Ji, Z.; Yaghi, O.M. A metal-organic framework of organic vertices and polyoxometalate linkers as a solid-state electrolyte. *J. Am. Chem. Soc.* **2019**, *141*, 17522–17526. [CrossRef]
86. Hasegawa, T.; Shimizu, K.; Seki, H.; Murakami, H.; Yoshida, S.; Yoza, K.; Nomiya, K. Polymerizable inorganic-organic hybrid: Syntheses and structures of mono-lacunary Dawson polyoxometalate-based olefin-containing organosilyl derivatives. *Inorg. Chem. Commun.* **2007**, *10*, 1140–1144. [CrossRef]
87. Hasegawa, T.; Murakami, H.; Shimizu, K.; Kasahara, Y.; Yoshida, S.; Kurashina, T.; Seki, H.; Nomiya, K. Formation of inorganic protonic-acid polymer via inorganic-organic hybridization: Synthesis and characterization of polymerizable olefinic organosilyl derivatives of mono-lacunary Dawson polyoxometalate. *Inorg. Chim. Acta* **2008**, *361*, 1385–1394. [CrossRef]
88. Nomiya, K.; Togashi, Y.; Kasahara, Y.; Aoki, S.; Seki, H.; Noguchi, M.; Yoshida, S. Synthesis and structure of Dawson polyoxometalate-based, multifunctional, inorganic-organic hybrid compounds: Organogermyl complexes with one terminal functional group and organosilyl analogues with two terminal functional groups. *Inorg. Chem.* **2011**, *50*, 9606–9619. [CrossRef]
89. Horan, J.L.; Genupur, A.; Ren, H.; Sikora, B.J.; Kuo, M.-C.; Meng, F.; Dec, S.F.; Haugen, G.M.; Yandrasits, M.A.; Hamrock, S.J.; et al. Copolymerization of divinylsilyl-11-silicotungstic acid with butyl acrylate and hexanediol diacrylate: Synthesis of a highly proton-conductive membrane for fuel-cell applications. *ChemSusChem* **2009**, *2*, 226–229. [CrossRef]

90. Horan, J.L.; Lingutla, A.; Ren, H.; Kuo, M.-C.; Sachdeva, S.; Yang, Y.; Seifert, S.; Greenlee, L.F.; Yandrasits, M.A.; Hamrock, S.J.; et al. Fast proton conduction facilitated by minimum water in a series of divinylsilyl-11-silicotungstic acid-*co*-butyl acrylate-*co*-hexanediol diacrylate polymers. *J. Phys. Chem. C* **2014**, *118*, 135–144. [CrossRef]
91. Motz, A.R.; Kuo, M.-C.; Horan, J.L.; Yadav, R.; Seifert, S.; Pandey, T.P.; Galioto, S.; Yang, Y.; Dale, N.V.; Hamrock, S.J.; et al. Heteropoly acid functionalized fluoroelastomer with outstanding chemical durability and performance for vehicular fuel cells. *Energy Environ. Sci.* **2018**, *11*, 1499–1509. [CrossRef]
92. Klaiber, A.; Landsmann, S.; Löffler, T.; Polarz, S. Fourfold action of surfactants with superacid head groups: Polyoxometalate-silicone nanocomposites as promising candidates for proton-conducting materials. *New J. Chem.* **2016**, *40*, 919–922. [CrossRef]
93. Lu, Z.-Q.; Zhang, L.-L.; Yan, Y.; Wang, W. Polyelectrolytes of inorganic polyoxometalates: Acids, salts, and complexes. *Macromolecules* **2021**, *54*, 6891–6900. [CrossRef]
94. Lu, Z.-Q.; Yin, Z.; Zhang, L.-L.; Yan, Y.; Jiang, Z.; Wu, H.; Wang, W. Synthesis of proton conductive copolymers of inorganic polyacid cluster polyelectrolytes and PEO bottlebrush polymers. *Macromolecules* **2022**, *55*, 3301–3310. [CrossRef]
95. He, H.; Zhu, Y.; Li, T.; Song, S.; Zhai, L.; Li, X.; Wu, L.; Li, H. Supramolecular anchoring of polyoxometalate amphiphiles into nafion nanophases for enhanced proton conduction. *ACS Nano* **2022**, *16*, 19240–19252. [CrossRef] [PubMed]
96. He, H.; Song, S.; Zhai, L.; Li, Z.; Wang, S.; Zuo, P.; Zhu, Y.; Li, H. Supramolecular modifying nafion with fluoroalkyl-functionalized polyoxometalate nanoclusters for high-selective proton conduction. *Angew. Chem. Int. Ed.* **2024**, *63*, e202409006. [CrossRef]
97. Konno, M.; Nakamura, M.; Aoyama, K.; Kogure, S.; Sato, H.; Kiyota, Y.; Misawa, T.; Kasuya, T.; Oda, Y.; Kinoshita, Y.; et al. Inorganic-organic crystalline synthetic bilayers consisting of polyoxomolybdate and double-chained surfactants. *Inorg. Chem. Commun.* **2020**, *117*, 107933. [CrossRef]
98. Li, H.; Qi, W.; Li, W.; Sun, H.; Bu, W.; Wu, L. A highly transparent and luminescent hybrid based on the copolymerization of surfactant-encapsulated polyoxometalate and methyl methacrylate. *Adv. Mater.* **2005**, *17*, 2688–2692. [CrossRef]
99. Ito, T.; Otobe, S.; Oda, T.; Kojima, T.; Ono, S.; Watanabe, M.; Kiyota, Y.; Misawa, T.; Koguchi, S.; Higuchi, M.; et al. Polymerizable ionic liquid crystals comprising polyoxometalate clusters toward inorganic-organic hybrid solid electrolytes. *Polymers* **2017**, *9*, 290. [CrossRef]
100. Ito, T.; Kiyota, Y.; Oda, T.; Watanabe, M.; Ono, S.; Oda, Y.; Misawa, T.; Isono, T.; Otobe, S.; Okamura, Y.; et al. Highly conductive polymer electrolytes constructed from polymerizable ionic liquid and inorganic cluster. *Trans. Mat. Res. Soc. Jpn.* **2019**, *44*, 101–107. [CrossRef]
101. Otobe, S.; Kiyota, Y.; Kojima, T.; Oda, Y.; Koguchi, S.; Okamura, Y.; Higuchi, M.; Kawano, M.; Nagase, Y.; Ito, T. Syntheses and structures of Keggin-type polyoxometalate crystals hybridized with a polymerizable ionic-liquid. *Trans. Mat. Res. Soc. Jpn.* **2021**, *46*, 15–18. [CrossRef]
102. Kobayashi, J.; Misawa, T.; Umeda, C.; Isono, T.; Ono, S.; Naruke, H.; Okamura, Y.; Koguchi, S.; Higuchi, M.; Nagase, Y.; et al. Controlled introduction of metal cations into polymerizable ionic liquid-polyoxomolybdate hybrid crystals. *CrystEngComm* **2019**, *21*, 629–636. [CrossRef]
103. Kiyota, Y.; Ono, S.; Sasaki, K.; Tamai, N.; Sugimoto, H.; Okamura, Y.; Koguchi, S.; Higuchi, M.; Nagase, Y.; Shinyashiki, N.; et al. Inorganic-organic hybrid crystals derived from polyoxovanadate and ionic-liquid toward promising conductive materials. *ChemNanoMat* **2024**, *10*, e202400188. [CrossRef]
104. Misawa, T.; Kobayashi, J.; Kiyota, Y.; Watanabe, M.; Ono, S.; Okamura, Y.; Koguchi, S.; Higuchi, M.; Nagase, Y.; Ito, T. Dimensional control in polyoxometalate crystals hybridized with amphiphilic polymerizable ionic liquids. *Materials* **2019**, *12*, 2283. [CrossRef] [PubMed]
105. Mikurube, K.; Hasegawa, K.; Matsumoto, T.; Kobayashi, J.; Naruke, H.; Ito, T. Isomerization-induced introduction of metal cations into polyoxomolybdate-surfactant hybrid crystals. *Inorg. Chem. Commun.* **2016**, *73*, 45–48. [CrossRef]
106. Kobayashi, J.; Shimura, K.; Mikurube, K.; Otobe, S.; Matsumoto, T.; Ishikawa, E.; Naruke, H.; Ito, T. Polyoxomolybdate layered crystals constructed from a heterocyclic surfactant: Syntheses, pseudopolymorphism and introduction of metal cations. *Materials* **2022**, *15*, 2429. [CrossRef]
107. Zou, K.; Deng, W.; Silvester, D.S.; Zou, G.; Hou, H.; Banks, C.E.; Li, L.; Hu, J.; Ji, X. Carbonyl chemistry for advanced electrochemical energy storage systems. *ACS Nano* **2024**, *18*, 19950–20000. [CrossRef]
108. Xu, L.; Li, S.; Tu, H.; Zhu, F.; Liu, H.; Deng, W.; Hu, J.; Zou, G.; Hou, H.; Ji, X. Molecular engineering of highly fluorinated carbon dots: Tailoring $Li^+$ dynamics and interfacial fluorination for stable solid lithium batteries. *ACS Nano* **2023**, *17*, 22082–22094. [CrossRef]
109. Peake, C.L.; Kibler, A.J.; Newton, G.N.; Walsh, D.A. Organic-inorganic hybrid polyoxotungstates as configurable charge carriers for high energy redox flow batteries. *ACS Appl. Energy Mater.* **2021**, *4*, 8765–8773. [CrossRef]

110. Amthor, S.; Knoll, S.; Heiland, M.; Zedler, L.; Li, C.; Nauroozi, D.; Tobaschus, W.; Mengele, A.K.; Anjass, M.; Schubert, U.S.; et al. A photosensitizer-polyoxometalate dyad that enables the decoupling of light and dark reactions for delayed on-demand solar hydrogen production. *Nat. Chem.* **2022**, *14*, 321–327. [CrossRef]
111. Zhang, G.; Li, X.; Chen, G.; Zhang, Y.; Wei, M.; Chen, X.; Li, B.; Wu, Y.; Wu, L. Supramolecular framework membrane for precise sieving of small molecules, nanoparticles and proteins. *Nat. Commun.* **2023**, *14*, 975. [CrossRef] [PubMed]

**Disclaimer/Publisher's Note:** The statements, opinions and data contained in all publications are solely those of the individual author(s) and contributor(s) and not of MDPI and/or the editor(s). MDPI and/or the editor(s) disclaim responsibility for any injury to people or property resulting from any ideas, methods, instructions or products referred to in the content.